Materials and Structures/Matériaux et Constructions, Vol. **34**, June 2001, pp 312-319

TECHNICAL REPORTS

Fracture and failure of thermally damaged concrete under tensile loading

B. E. Barragán[1, 2], G. M. Giaccio[3, 4] and R. L. Zerbino[1, 3]

(1) National Council of Scientific and Technological Research, CONICET, La Plata, Argentina

(2) ETSECCPB, UPC, Barcelona, Spain

(3) UNLP (University of La Plata), Department of Civil Engineering, La Plata, Argentina

(4) CIC-LEMIT, Commission of Scientific Research, La Plata, Argentina

Paper received: May 26, 2000; Paper accepted: January 2, 2001

ABSTRACT

Concrete is a brittle composite material where the failure mechanism is closely related to the initiation and propagation of cracks. The presence of microcracks and other defects in concrete allows, unlike in the case of an ideal brittle material, the existence of a failure process that includes the branching and bifurcation of the cracks, which gives rise to the appearance of an inelastic behavior and then to a higher energy consumption during failure and an extension of the zone in which fracture takes place. This work studies the failure behavior of damaged concretes in tension and compares the behavior of concrete of different strength levels and component materials when adopting temperature as the damaging tool. Two water / cement ratios, two types of coarse aggregates and the incorporation of natural pozzolans are included as variables. As a way to evaluate the damage produced in the internal structure of concrete, the dynamic modulus of elasticity was measured on each specimen. Measures of strength, deformability, and fracture energy determined over notched prisms are reported. In a complementary way, the results of compression tests (strength, static modulus of elasticity, and Poisson ratio) over cylindrical specimens are included.

RÉSUMÉ

Le béton est un matériau composite fragile dans lequel le mécanisme de rupture est étroitement lié à un processus de formation et de propagation des fissures. La présence de microfissures et autres défauts dans le béton conduit, contrairement à ce qui se passe pour un matériau fragile idéal, à l'existence d'un processus de rupture qui comprend ramification et bifurcation des fissures, ce qui donne lieu à l'apparition d'un comportement inélastique ; ceci entraîne une plus grande consommation d'énergie pendant la rupture ainsi qu'une extension de la zone dans laquelle s'est produite la fracture. Dans ce travail, on étudie le mécanisme de rupture de bétons endommagés sous des sollicitations de traction. On a adopté la température comme instrument d'endommagement en comparant le comportement de bétons ayant des résistances ainsi que des matériaux constitutifs différents. Les variables sont deux rapports eau/ciment différents, deux types de gros granulats et l'incorporation d'une pouzzolane naturelle. Afin d'évaluer les dommages produits dans la structure interne du béton, le module d'élasticité dynamique a été mesuré dans chaque éprouvette. La résistance, la déformabilité et l'énergie de fracture se mesurent à l'aide d'éprouvettes prismatiques entaillées. À titre complémentaire sont rapportés les résultats de tests de compression obtenus avec des cylindres (résistance, module d'élasticité statique et coefficient de Poisson).

1. INTRODUCTION

Concrete is a composite material where inclusions of different size and shape, the aggregates, are surrounded by a more or less continuous matrix that acts like a binder. This matrix, regarding the observation level could be cement paste or mortar. It includes diverse types of defects (pores, microcracks). Like in other brittle materials, the failure mechanism of concrete is closely related to the initiation and propagation of cracks. Coarse aggregates generate weaker zones (interfaces) in which the development of the cracks begins. Numerous works verified the microstructure and morphological differences of the interfaces with respect to the paste [1]. Furthermore, macrodefects generated during compaction, bleeding, etc. may concentrate around the bigger aggregates and also cracks will appear due to different stiffnesses, shrinkage or thermal expansion coefficients between paste and aggregates.

The presence of microcracks and other defects in concrete allows, unlike in the case of an ideal brittle material, the occurrence of different failure processes that includes

Editorial Note
The UPC is a RILEM Titular Member.

the branching and bifurcation of the cracks, which gives rise to the appearance of an inelastic behavior, and which leads to a higher energy consumption during failure and an extension of the zone in which fracture takes place [2-3]. The reduction of the level of defects has been the way through which the high-strength grade has been achieved in concrete, nevertheless, it is known that an increase in the relative brittleness of these concretes is also produced [4].

An important case of damage of the structure of concrete appears when it is exposed to high temperatures. The different dilatation coefficients of the phases of the composite and the changes in water content of the cement paste produce cracks. Initially, the temperature elevation results in the elimination of the water contained in the pore system and the consequent contraction of the paste with crack formation. Temperature rise over 500°C produces an alteration in concrete that can be considered non-reversible, as the loss of chemical bounded water (dehydration of the paste) takes place. The difference between the thermal dilatation coefficients of the aggregates with respect to the paste causes microcracking at the interfaces, which increases the size and closeness of the internal cracks.

Diverse works have verified the degradation of the microstructure due to the exposure to high temperatures and its effects over the behavior of concrete, the changes being a function of the heating and cooling cycle [5-14]. Most of the studies refer to its effects over the compression behavior reporting reductions in the ultrasonic pulse velocity, the dynamic modulus of elasticity, strength, etc. Evaluation of the tensile strength shows a great variability, and it is verified that it is more sensitive than the compression strength to the changes produced by the exposure to high temperatures, with the type of aggregate being of great importance. Recent studies on the residual properties in flexure and direct tension of high-strength concretes exposed to high temperature verify the decrease in tensile strength and toughness, the increase in characteristic length, and only minor effects on the fracture energy [15].

The objective of this work is to study the failure behavior of damaged concretes in tension. Temperature was adopted as the damaging tool, comparing the behavior of concrete series including different strength levels and different component materials. Measures of strength, deformability, and fracture energy determined over notched prisms are reported. In complementary way, the results of compression tests (strength, static modulus of elasticity, and Poisson ratio) of cylindrical specimens are included. With the aim of determining whether the alterations in specimens of different geometry were similar, the dynamic modulus of elasticity was measured previous to the compression and tension tests.

2. EXPERIMENTAL

2.1 Specimen composition and heat treatment

Different levels of defects were introduced in concrete through the exposure to high temperatures, varying the maximum temperature and the cooling rate. Then, alterations in the interface zones and some degrees of cracking of the matrix can be foreseen. Five series of concretes with different strength levels and type of coarse aggregate are analyzed.

Concretes with water/cement ratios equal to 0.33 and 0.50 were elaborated using normal Portland cement, siliceous river sand, and 19-mm maximum size granitic crushed stone as coarse aggregate (0.33-0-CS and 0.50-0-CS). Through the replacement of 15% of the cement by a natural pozzolan, concretes 0.33-15-CS and 0.50-15-CS were obtained. Also, a w/c = 0.50 concrete was prepared using a 19 mm maximum size river gravel as coarse aggregate (0.50-0-RG).

Cylinders of 150 × 300 mm and prisms of 75 × 105 × 430 mm were cast. In each case, a group of specimens was maintained as reference concrete (Control) and other groups were exposed to temperatures of 500 and 700°C, and then cooled under different conditions. A detailed analysis of the effects of high temperatures over the stress-strain behavior of concrete under compression loads has previously been done [16-17].

The curing and the exposure process are summarized as follows. To attain uniform curing conditions and avoid the superposition of other factors (different hydration rates, moisture conditions, etc.) on the effect of high temperatures, all specimens were cured for 28 days in a fog room (RH: 95%, T: 20 ± 2°C) and then stored for another 28 days in the laboratory environment prior to heating. The specimens were exposed to temperatures of 500 or 700°C for a period of one hour; then they were cooled by two different procedures: a- slowly, (they were allowed to cool by themselves in the interior of the oven) and w- fast, (they were taken out of the oven immediately after the established time was completed and then cooled by water spurts for a minimum time of half an hour). In this way, different grades of residual damage were obtained. After the exposure, the specimens were maintained subsequently for 7 days in the laboratory to attain uniform humidity conditions in specimens cooled with air and water.

2.2 Test methods

As a way to evaluate the structure of the material the dynamic modulus of elasticity was measured on cylinders and prisms (before the notch was cut). In this way it was possible to estimate if the damage level was similar in specimens of different shape. The longitudinal resonant frequency was obtained using electronic equipment with a frequency range that can oscillate between 10 Hz and 100 kHz.

The compression strength, static modulus of elasticity, and Poisson's ratio were measured on the cylinders. The stress-strain behavior was determined using LVDTs for measuring longitudinal and lateral deformations. Load ramps up to 40% of the maximum load were applied.

For the study of the stress-strain behavior in tension, three-point bending tests of middle notched specimens were performed in a displacement controlled testing

Table 1 – Residual properties measured on cylinders

CONCRETE		E_d (GPa)	(%)	f_c (MPa)	(%)	E (GPa)	(%)	μ	(%)
0.50-0-CS	Control	42.0	100	37.5	100	36.4	100	0.16	100
	500-a	13.7	33	33.4	89	15.5	43	0.10	62
	500-w	8.6	20	22.4	60	11.0	30	0.03	19
	700-w	2.9	7	16.3	43	3.9	11	0.04	25
0.33-0-CS	Control	46.4	100	51.6	100	40.0	100	0.19	100
	500-a	20.2	44	43.6	84	23.3	58	0.12	63
	500-w	14.8	32	38.9	75	22.9	57	0.08	42
0.50-0-RG	Control	41.9	100	30.0	100	38.6	100	0.16	100
	500-a	12.7	30	23.9	80	18.2	47	0.10	62
	500-w	8.3	20	18.5	62	15.3	40	0.02	12
0.50-15-CS	Control	42.4	100	39.0	100	36.6	100	0.18	100
	500-a	20.1	47	37.1	95	20.8	57	0.12	67
	500-w	21.1	50	30.6	78	18.3	50	0.08	44
0.33-15-CS	Control	46.2	100	56.0	100	40.7	100	0.18	100
	500-a	26.4	57	53.7	96	27.5	68	0.10	56
	500-w	18.6	40	40.9	73	25.6	63	0.08	44
	700-a	4.3	9	27.5	49	8.6	21	0.07	39
	700-w	3.1	7	20.7	37	5.8	14	0.03	17

machine (Instron 150 kN) following the general guidelines of RILEM Technical Committee 50-FMC [18]. The notch was cut up to a depth equal to half of the beam's height and performed after the thermal treatment using a diamond saw. The beams were loaded over a span of 315 mm with a rate of 0.2 mm/min, measuring the central deflection by means of LVDT. The load-deflection curve and the values of the net bending stress at maximum load (f_{net}) and the energy of fracture (G_F) were obtained.

The energy of fracture is calculated as $G_F = W_0 + mg\delta_0 / A_{lig}$, where W_0 is the area below the curve, $mg\delta_0$ the contribution of the weight of the beam, δ_0 the displacement at the final fracture of the beam, mg the weight (between the supports), and A_{lig} the cross-sectional area of the ligament.

The net bending stress at maximum load is calculated as $f_{net} = 6 (F_{max} + (mg/2)).l / 4bh^2$ where b is the width of the beam, h the net depth of the beam, l the span and F_{max} the maximum load.

Finally, after the flexural tests, the splitting tensile strength (f_s) was measured over the broken halves of the beams.

3. RESULTS

Table 1 presents the results of the dynamic (E_d) and static (E) modulus of elasticity, compressive strength (f_c), and the Poisson coefficient (μ) obtained from 150 x 300 mm cylinders. Absolute values, as well as the percentage with respect to the reference concrete, are given.

Fig. 1 shows, for each series and all exposure conditions, the load-deflection curve corresponding to the specimen which best fits the average value. In the case of affected specimens a notable strength decrease and a higher deformability can be observed. The non-linear response indicates the existence of cracks with an advanced grade of propagation from the initial stages of the test, being remarked as the test advances. Regarding the fracture surface, it is interesting to note that while in undamaged concretes (Control) the crack originates at the tip of the notch and propagates towards the loading point, in many tests of damaged concretes it was observed that the crack propagates away from the central plane of the specimen, sometimes more than 20 mm, resulting a more tortuous fracture surface.

Table 2 shows the values of the residual dynamic modulus of elasticity (E_d) of prisms, the residual net bending strength (f_{net}), the residual

Table 2 – Residual properties measured on prisms

CONCRETE		E_d (GPa)	(%)	f_s (MPa)	(%)	f_{net} (MPa)	(%)	G_F (N/m)	(%)	δ_0 (mm)	(%)	l_{ch}	(%)
0.50-0-CS	Control	47.4	100	3.8	100	6.1	100	230	100	1.6	100	580	100
	500-a	12.6	27	1.6	42	2.1	34	135	59	1.6	100	817	141
	500-w	9.6	20	1.8	47	2.0	33	200	87	2.4	150	679	117
	700-w	2.0	4	0.8	21	1.2	20	140	61	2.0	125	853	147
0.33-0-CS	Control	50.3	100	4.2	100	7.6	100	210	100	1.3	100	476	100
	500-a	23.7	47	2.9	69	4.2	55	301	143	2.8	215	834	175
	500-w	19.2	38	2.8	67	4.2	55	255	121	2.0	154	745	156
0.50-0-RG	Control	47.2	100	3.3	100	5.7	100	185	100	1.5	100	656	100
	500-a	17.0	36	2.2	67	3.0	53	140	76	1.4	93	526	80
	500-w	16.4	35	2.1	64	3.0	53	165	89	2.0	133	572	87
0.50-15-CS	Control	44.8	100	3.8	100	7.0	100	207	100	1.4	100	525	100
	500-a	13.3	30	1.8	47	3.2	46	192	93	1.9	136	1233	235
	500-w	13.8	31	2.3	61	3.1	44	199	96	1.9	136	688	131
0.33-15-CS	Control	50.2	100	4.2	100	7.8	100	220	100	1.4	100	508	100
	500-a	26.0	52	2.8	67	5.8	74	275	125	2.1	150	965	190
	500-w	25.1	50	2.6	62	5.5	71	260	118	2.0	143	985	194
	700-a	3.8	8	1.1	26	1.5	19	175	80	2.4	171	1244	245
	700-w	4.1	8	1.3	31	2.0	26	200	91	2.6	186	686	135

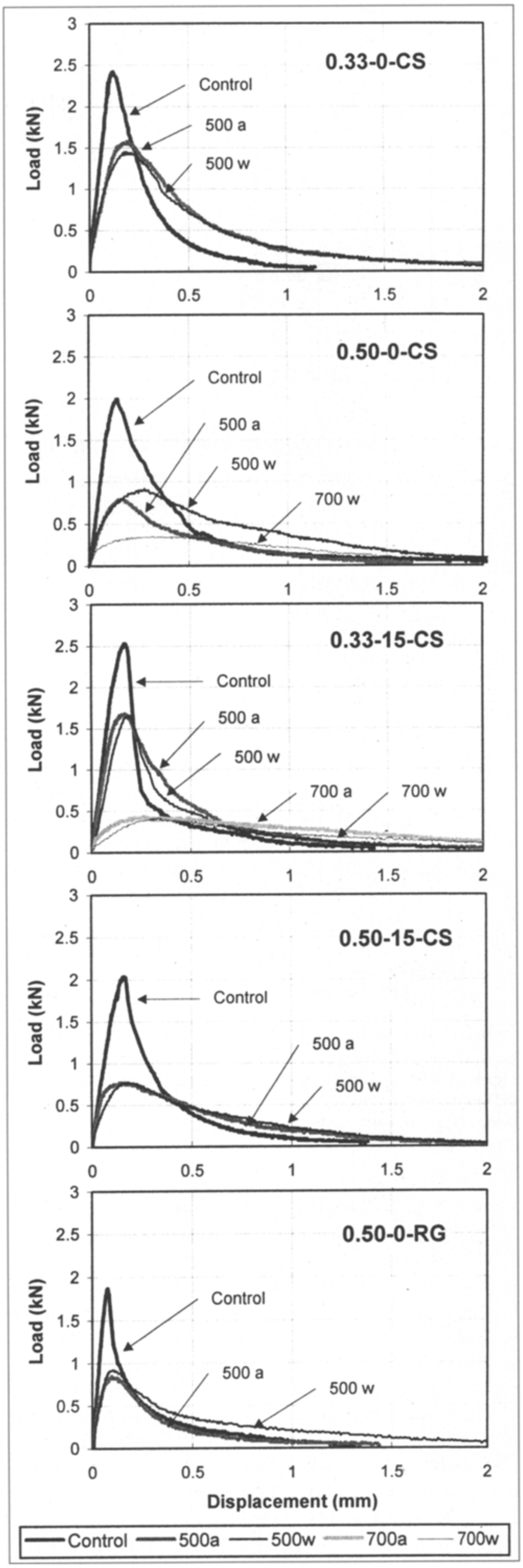

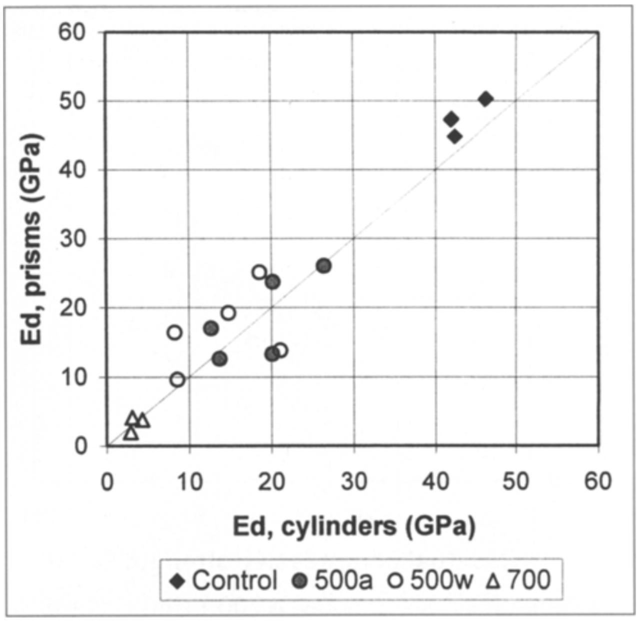

Fig. 2 – Comparison between the residual dynamic modulus of elasticity measured on cylinders and prisms.

energy of fracture (G_F), the residual characteristic length ($l_{ch} = E \cdot G_F / f_s^2$) , and the final displacement (δ_0) obtained from the flexure tests. It also presents the results of the residual splitting tensile strength (f_s) obtained afterwards from the halves of the beams. As in the case of compression, the absolute values and the percentages with respect to the reference concrete are included.

It must be noted that for exposure temperatures of 700°C, the river gravel specimens suffered such a level of damage that there was no sense to evaluate its properties.

4. DISCUSSION

The residual dynamic modulus of elasticity (Tables 1 and 2) is significantly reduced with temperature, pointing out the alteration in the internal structure of concrete. The relation between the measured values on cylinders and prisms is presented in Fig. 2. It can be seen that the plots are located very near the equality line, indicating that the level of damage of the internal structure of the material is similar for both types of specimens.

Considering the compressive tests, a decrease in residual strength and stiffness appears, the latter being much more significant (Fig. 3). As an example, for 500°C and slow cooling, the residual static modulus of elasticity shows a reduction of a 40%, while the strength decrease does not exceed 20%. For temperatures of 700°C, the damage is such that, in the case of granitic crushed stone concretes, the residual values of the modulus of elasticity and strength are in the order of 15 and 40%, respectively.

Fig. 1 – Load – displacement curves.

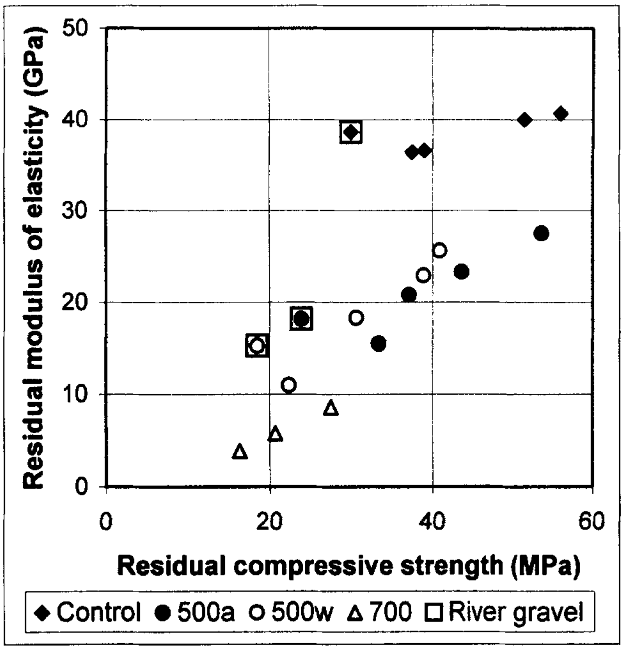

Fig. 3 – Residual static modulus of elasticity vs. residual compressive strength.

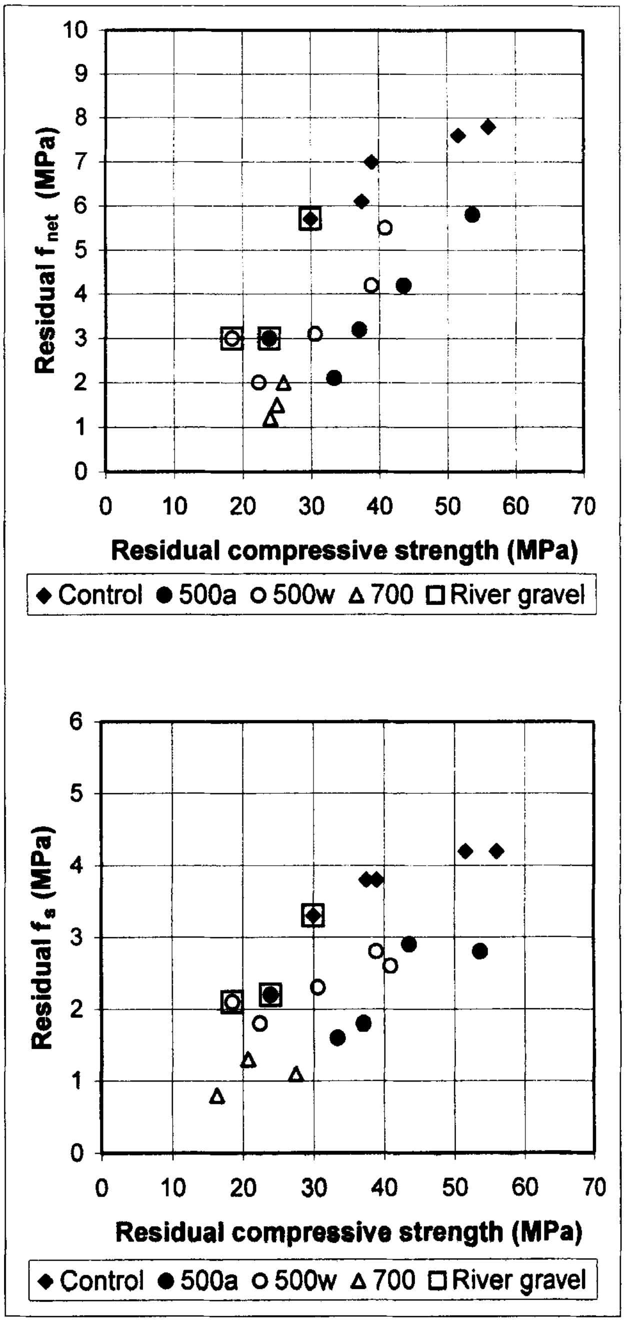

Fig. 4 – Variation of the residual tensile strength with the residual compressive strength, a) modulus of rupture of notched beams (f_{net}), b) splitting test (f_s).

The residual Poisson ratio notably decreases, reflecting the generalized presence of internal cracks that modify their size as load is applied. It can be observed that the decreases in the Poisson coefficient (Table 1) are much more important in the case of specimens cooled by water spurts. Fig. 3 shows the relationship between the static modulus of elasticity (E) and the compressive strength (f_c). It can be seen that there are significant changes in the relationship between residual static modulus of elasticity (E) and the residual compressive strength (f_c) of thermally damaged concretes. However, the study of the behavior and failure mechanism under compression loads is out of the scope of this work, and some considerations about the theme and limitations of the use of expressions for estimating the modulus of elasticity based on f_c have been previously published [17].

Figs. 4a and 4b show the relationship between compressive and tensile strength. The behavior under tensile loads (Table 2) is consistent with the one observed in compression, but residual tensile strength seems to be more affected by cracking than the residual compressive strength. This is verified for the different concretes and for both types of aggregates, no matter if the tensile strength is determined through the splitting or the flexure test. In the case of crushed stone concrete 0.50-0-CS, the reductions in strength were higher than for the river gravel concrete 0.50-0-RG; moreover, the residual strength of the former was even lower in absolute terms. In this crushed stone concrete, the exposure at 500°C decreased the residual modulus of rupture and the residual splitting tensile strength to a mean of 33 and 45% respectively with respect to the reference concrete, while in the case of the river gravel concretes, those same percentages were equal to 53 and 65%. The presence of pozzolans did not strongly modify tensile strength; however, the tendency is for concrete with pozzolans to have higher residual values. It is also possible to note that there is practically no difference in residual tensile strength derived from the type of cooling.

Figs. 5a and 5b show respectively, the variation of the relations f_{net}/f_c and f_s/f_c with the residual compressive strength; as it was mentioned earlier while residual tensile strength has not been significantly affected by cooling rate, residual compressive strength has (Tables 1 and 2), then a difference in these relationships appears, and it is possible to appreciate that they decrease in the case of damaged concretes. After cooling different type of cracking appeared at the surface of the specimens. In the case of high cooling rate, wide and localized cracks (detectable at simple view) were observed on the surface.

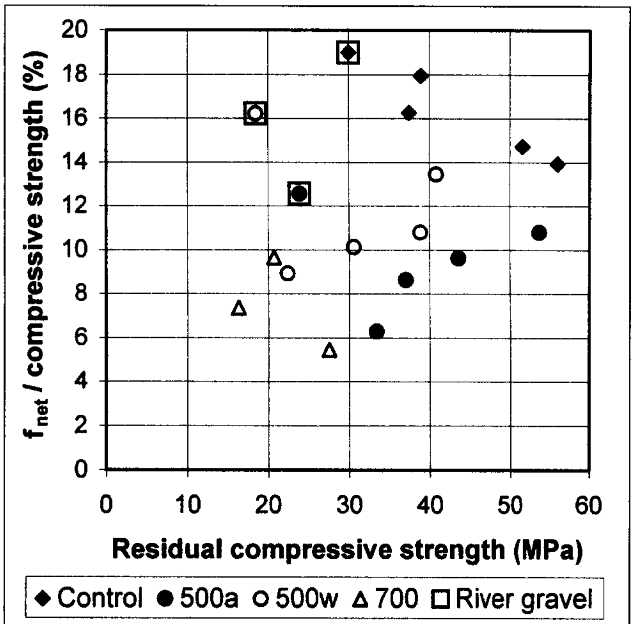

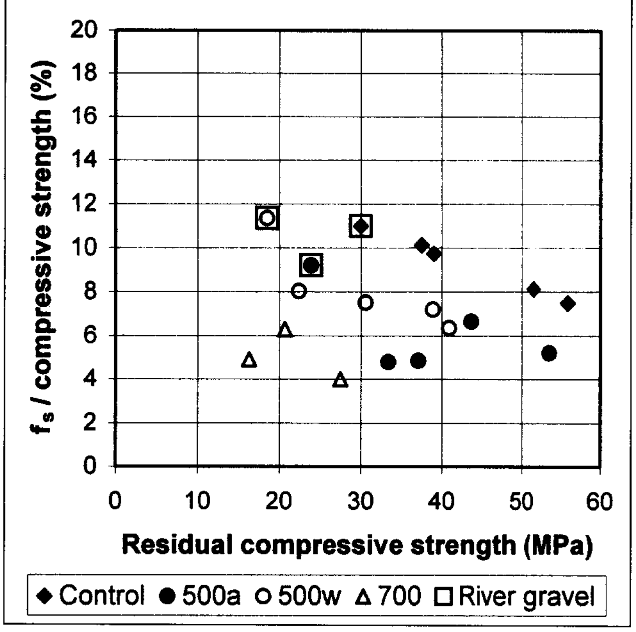

Fig. 5 – Variation of the residual tensile / compressive strength ratios with the residual compressive strength, a) modulus of rupture of notched beams (f_{net}), b) splitting test (f_s).

Crack widths higher than 0.50 mm were measured. While a lower cooling rate was used, no wide localized cracks were seen. Crack width was quite smaller, most fissures were in the order of 0.05 mm, and only a few exceptions achieved 0.10 mm. Based on these observations, the different effect of cooling rate on compressive and tensile strength, as observed in Fig. 5, can be explained assuming as a hypothesis that a distinct type of cracking appears: a high rate of cooling can cause the appearance of wider and localized cracks, while a lower cooling rate produces a more generalized microcracking. This hypothesis is coherent with the differences previously mentioned in the Poisson coefficient for the different types of cooling.

The degradation of the structure notably affects the way in which cracks propagate. As it was observed in Fig. 1, microcracking produces changes in the shape of the curves at the pre- and post-peak stages. While unaffected concretes show a practically linear behavior up to the peak load, concretes exposed to high temperature modify their stiffness along the ascending branch. Sometimes the deformation at peak load is less defined due to a plateau type behavior and a much smoother slope of the softening branch.

In the case of microcracked concrete the post-peak regime has stronger incidence on the measurements of the fracture energy than sound concrete. While damage produces a drop in strength (f_{net}) the reduction of the fracture energy (G_F) is not so important due to the greater branching in crack propagation (see Table 2). In this way an increase in G_F could even exist in some cases. The microcracking extended along the matrix and the interfaces is responsible for a higher amount of energy consumed during the failure process. An example of these are the high strength concretes exposed to 500°C, where the tensile strength decreases to residual values between 55 and 70%, but at the same time, an increase in values of G_F is measured. An increase in the energy of fracture in high strength concretes affected by high temperatures was also found by Felicetti and Gambarova [15].

Fig. 6 shows the variation of residual fracture energy with the compressive strength. As it was mentioned above, while a decrease in strength appears as the previous crack increases, the presence of the defects enhances the development of a more tortuous and erratic crack pattern. Depending on which of these two effects dominates, the energy values can either grow or diminish. Comparing the results obtained with both types of aggregate can also show that while in the case of river gravel the energy of fracture of damaged concretes

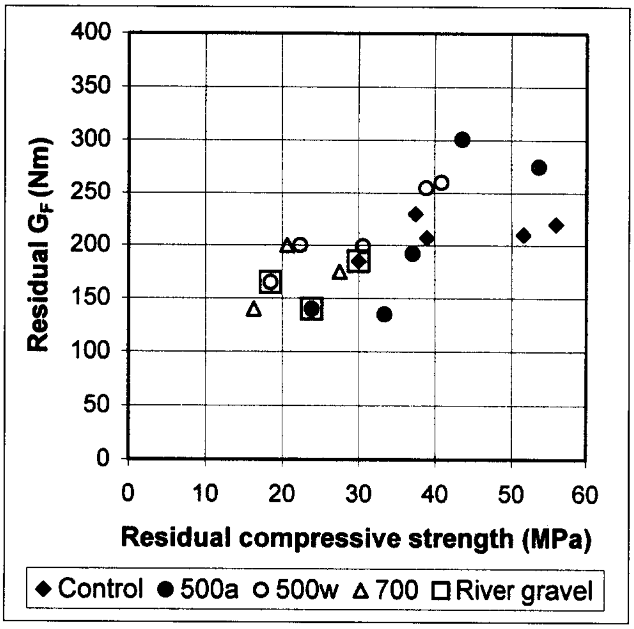

Fig. 6 – Variation of the residual energy of fracture (G_F) with the residual compressive strength.

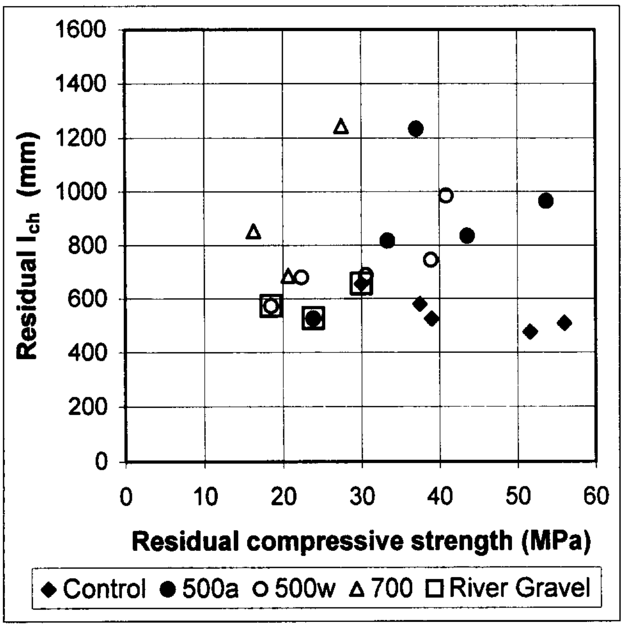

Fig. 7 – Variation of the residual characteristic length (l_{ch}) with the residual compressive strength.

always decreased, in concretes prepared with crushed stone G_F usually tends to increase. This can be explained by the characteristics of the coarse aggregate. In the case of a rough, irregular and good bonding aggregate that improves crack branching (as the used crushed stone), the effect of energy increase due to the growth of the cracking level seems more relevant than the strength decrease. On the contrary, when a smooth, round and low bond aggregate is used (which is the case of this river gravel) the crack branching increase is not important enough to compense the strength decrease. As strength level increases these influences will be more relevant. An analysis of the effect of coarse aggregate characteristics on the failure mechanism of conventional and high strength concretes has been presented before [19].

In Fig. 7, the characteristic length versus the compressive strength is represented. The residual characteristic length is significantly higher in the case of pre-cracked concretes. The damaging of the material increases the size of the fracture process zone, reducing the brittleness of concrete (the relation G_F/f_c, is higher in affected concretes). In damaged concretes, the characteristic length can be even double the control values. A different behavior appears when analyzing concretes made with river gravel. In this case the fracture process zone is not greatly modified when exposed to high temperature, and the results can even be smaller than the Control ones.

It is known that final deflections depend on the type and size of the coarse aggregate, and these tend to decrease with the strength level. The results of Table 2 show that final deflections increase in damaged concretes. In some cases differences regarding the type of cooling appeared, they might depend on the type and level of damage in the surroundings of the notch.

5. CONCLUSIONS

This work studied the failure residual behavior of damaged concretes of different strength levels and component materials. A temperature cycle was adopted as the damaging tool and the residual dynamic modulus of elasticity was measured as a way to evaluate the degree of alteration of the internal structure of concrete. The following conclusions can be drawn:

The measurements of the residual dynamic modulus of elasticity indicate that the level of damage of the internal structure of the material is similar for both types of specimens used in flexural and compressive tests.

The residual tensile strength appears to be more affected by the cracking than the compression strength. This is verified for the different concretes, regardless if the tensile strength is determined through the splitting or the flexure test.

It is verified that the presence of microcracking causes a greater decrease in residual stiffness than in residual compressive strength.

The degradation of the structure notably affects the way in which cracks propagate and this is reflected in the shape (ascending and softening) of the load-deflection curves. A strong incidence of the post-peak regime exists on the measurements of the fracture energy. While damage produces a drop in strength the reduction of the fracture energy is less important due to the greater branching in crack propagation, and even an increase in the energy appeared in some damaged concretes.

Considering concrete composition, the energy was lower in concretes containing round shaped and low adhesion particles, but it must be noted that compared with the unaffected series in normal strength concrete, the energy changes were of similar order for both types of aggregates. Comparing concretes prepared with granitic crushed stone it can be seen that as strength level increases, the presence of cracking produces an increase in the residual energy of fracture, except in the case of highly damaged concretes (700°C).

Regarding the size of the fracture process zone, the residual characteristic length is significantly higher in the case of pre-cracked concretes prepared with crushed stone. In the case of concretes made with river gravel the residual characteristic length is not greatly modified.

REFERENCES

[1] 'Interfaces in cementitious composites', Proceedings of the RILEM Int. Conf E & FN SPON (J. C. Maso, LMDC, INSA-UPS, Toulouse, France, 1992).

[2] Mehta, P. K. and Monteiro, P. J. M., 'Concrete: Structure, Properties and Materials', (Prentice Hall, NJ, 1993).

[3] Ziegeldorf, S., 'Phenomenological aspects of the fracture of concrete', in 'Fracture Mechanics of Concrete', (F.H. Wittmann, Elsevier, NY 1983) 31-41.

[4] Giaccio, G., Rocco, C. and Zerbino, R., 'The fracture energy (G_F) of high strength concretes', *Mater. Struct.* **26** (161) (1993) 381-386.

[5] Bažant, Z. and Kaplan, M., 'Concrete at high temperatures', (Longman, First edition, Essex, UK, 1996).

[6] Abrams, M. S., 'Compressive strength of concrete at temperatures to 1600°F', in 'Temperature and Concrete', ACI SP-25 (American Concrete Institute, Detroit, 1971) 33-58.
[7] Zoldners, N. G., Malhotra, V. M. and Wilson, H. C. 'Effect of high temperature on concretes incorporating different aggregates', *ASTM J.* **60** (1960) 1087-1108.
[8] 'Concrete for Nuclear Reactors', ACI SP-34 (American Concrete Institute, Detroit, 1972).
[9] RILEM TC-129 MHT, 'Test methods for mechanical properties of concrete at high temperatures: Compressive strength for service and accident conditions', *Mater. Struct.* **28** (181) (1995) 410-414.
[10] RILEM TC-129 MHT, 'Test methods for mechanical properties of concrete at high temperatures: Tensile strength for service and accident conditions', *Mater. Struct.* **33** (228) (2000) 219-223.
[11] Baker, G., 'The effect of exposure to elevated temperatures on the fracture energy of plain concrete', *Mater. Struct.* **29** (190) (1996) 383-388.
[12] Papayianni, M. and Valiasis, T., 'Residual mechanical properties of heated concrete incorporating different pozzolanic materials', *Mater. Struct.* **24** (140) (1991) 115-121.
[13] Zhang, B., Bicanic, N., Pearce, C. J. and Balabanic, G., 'Residual fracture properties of normal- and high-strength concrete subjected to elevated temperatures', *Magazine of Concrete Research* **52** (2) (2000) 123-136.
[14] Mohamedbhai, G. T .G., 'Effect of exposure time and rates of heating and cooling on residual strength of heated concrete', *Magazine of Concrete Research* **38** (136) (1986) 151-158.
[15] Felicetti, R. and Gambarova, P. G., 'On the residual tensile properties of high performance siliceous concrete exposed to high temperature', in the Proceedings of the International Workshop in honor of Z. P. Bažant's Anniversary (Prague, 1998) 1-20.
[16] Barragán, B., Di Maio, A., Giaccio, G., Traversa, L. and Zerbino, R., 'Effects of high temperature on residual mechanical and transport properties of concrete', Proceedings of the Fifth CANMET/ACI International Conference on Durability of Concrete, ACI SP-192 (American Concrete Institute, Barcelona, 2000) 983-1000.
[17] Di Maio, A., Giaccio, G. and Zerbino, R., 'Relationship between the static and dynamic modulus of elasticity of concretes exposed to high temperatures', Proceedings of the V Iberoamerican Congress of Construction Pathologies and VII Congress of Quality Control (Montevideo, 1999) 331-338. (Only available in Spanish).
[18] RILEM TC-50 FMC, 'Determination of the fracture energy of mortar and concrete by means of three-point bend tests on notched beams', *Mater. Struct.* **18** (106) (1985) 285-290.
[19] Giaccio, G. and Zerbino, R., 'Failure mechanism of concrete: Combined effects of coarse aggregates and strength level', *Advanced Cement Based Materials* **7** (1) (1998) 41-48.